5358 *Biochemistry* **2009,** *48,* 5358–5364
DOI: 10.1021/bi900128e

BIOCHEMISTRY
including biophysical chemistry & molecular biology
Article

Small-Molecule Suppression of Misfolding of Mutated Human Carbonic Anhydrase II Linked to Marble Brain Disease[†]

Karin Almstedt,[‡] Therese Rafstedt,[‡] Claudiu T. Supuran,[§] Uno Carlsson,[‡] and Per Hammarström*[,‡]

[‡]*IFM-Department of Chemistry, Linköping University, 581 83 Linköping, Sweden, and* [§]*Polo Scientifico, Laboratorio di Chimica Bioinorganica, Università deli Studi di Firenze, Florence, Italy*

Received January 27, 2009; Revised Manuscript Received April 29, 2009

ABSTRACT: Carbonic anhydrase II deficiency syndrome or Marble brain disease (MBD) is caused by autosomal recessive mutations in the human carbonic anhydrase II (HCA II) gene. Here we report a small-molecule stabilization study of the exceptionally destabilized HCA II mutant H107Y employing inhibitors based on *p*-aminobenzoylsulfonamide compounds and 1,3,4-thiadiazolylsulfonamides as well as amino acid activators. Protein stability assays showed a significant stabilization by the aromatic sulfonamide inhibitors when present at 10 μM concentration, providing shifts of the midpoint of thermal denaturation between 10 °C and 16 °C and increasing the free energies of denaturation 0.5−3.0 kcal/mol as deduced from GuHCl denaturation. This study could be used as a starting point for the design of small-molecule folding modulators and possibly autoactivatable molecules for suppression of misfolding of destabilized HCA II mutants.

A wide spectrum of metabolic and degenerative diseases is caused by misfolding of crucial enzymes (*1*). In most cases these are autosomal recessive inherited diseases. In humans the enzyme carbonic anhydrase II is present in red blood cells, kidney, osteoclasts, choroid plexus, and glial cells of the brain. Human carbonic anhydrase II (HCA II)[1] catalyzes the hydration of carbon dioxide into hydrogen carbonate at an astonishing rate with a turnover of 10^6 molecules/s (*2*−*4*). HCA II is an enzyme important for a plethora of pH homeostasis functions of diverse cell types including respiration, generation of cerebrospinal fluid, for bone resorption, and kidney filtration. Carbonic anhydrase II deficiency syndrome (CADS) is an autosomal recessive disease presenting with diverse symptoms reflecting loss of HCA II functions: renal tubular acidosis, osteopetrosis, dental malocclusion, optic nerve compression, and mental retardation. Linkage of the HCA II gene to the disease was elucidated through the fact that HCA II was the only known CA isozyme expressed both in kidney and in brain. Furthermore, side effects of known carbonic anhydrase inhibitors (CAIs) presented some treated patients with renal tubular acidosis, induced calcium release from bone, and reduced CSF production (*5*).

HCA II is composed of 259 amino acids, where the funnel-shaped active site is buried in the center of the molecule. In the active site a Zn^{2+} ion is liganded to three histidines (H94, H94, and H119). The protein structure is mainly folded into a large extensive twisted β-sheet, with 10 mainly antiparallel strands building the framework of the protein spanning the entire molecule (*6*). Several mutations in the HCA II gene are known to induce CADS (*7*), several of which are missense point mutations, and others induce early termination or frame shifts. The first point mutation in CADS discovered was the His107Tyr (H107Y) mutation in an Italian American family (*8*), which was later also found in a Japanese family (*9*). We have previously deciphered the misfolding mechanism of the H107Y point mutation linked to CADS and have shown that the mutant is misfolded under physiological conditions, i.e., 37 °C, whereas the protein is competent to fold at low temperatures (*10*). A previously important observation from our studies of HCA II mutations in position 107 revealed a transition-like dependence on the midpoint of thermal denaturation (T_m) versus yield of native recombinant protein (*11*). In humans carrying the HCA II_{H107Y} CADS mutation revealed the absence of HCA II in erythrocytes indicating that the mutant was efficiently degraded within the cell (*5*). Employing the well-known small-molecule inhibitor acetazolamide, we have demonstrated that the folding equilibrium can be shifted toward correctly folded HCA II_{H107Y}. Long-term treatment with acetazolamide has been associated with symptoms such as metabolic acidosis (*12*). Other CAIs have been extensively explored for treatment of a variety of conditions.

[†]This work was supported by the Swedish Research Council (U.C., P.H.), the Knut and Alice Wallenberg Foundation (P.H., U.C.), and The Swedish Foundation for Strategic Research (P.H.). P.H. is a Swedish Royal Academy of Science Research Fellow sponsored by a grant from the Knut and Alice Wallenberg Foundation. Research from the laboratory of C.T.S. was financed by an EU grant of the sixth framework programme (DeZnIT project) and by an Italian FIRB project (MIUR/FIRB RBNE03PX83_001).

*Corresponding author. Phone: (46)-13-285690. Fax: (46)-13-281399. E-mail: perha@ifm.liu.se.

[1]Abbreviations: CADS, carbonic anhydrase II deficiency syndrome; CAI, carbonic anhydrase inhibitor; GuHCl, guanidine hydrochloride; HCA II, human carbonic anhydrase II; HCA II_{H107Y}, mutated human carbonic anhydrase II with a tyrosine for histidine substitution in position 107.

 Published on Web 05/05/2009

Table 1: IC_{50} Values of Compounds **1**−**9** on HCA II and HCA II_{H107Y}

Comp.#	Structure	Name	IC_{50} (H107Y) nM	IC_{50} (HCA II) nM
1	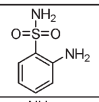	2-Amino-benzenesulfonamide	248	235
2	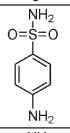	4-Amino-benzenesulfonamide	60	43
3	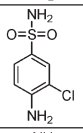	4-Amino-3-chloro-benzenesulfonamide	70	65
4	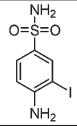	4-Amino-3-iodo-benzenesulfonamide	145	80
5	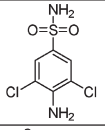	4-Amino-3,5-dichloro-benzenesulfonamide	1640	553
6	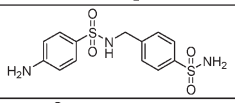	4-Amino-N-(4-sulfamoylbenzyl)-benzenesulfonamide	13	6
7	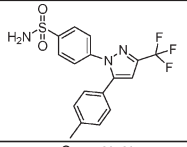	4-(5-p-Tolyl-3-trifluoromethyl-pyrazol-1-yl)-benzenesulfonamide (Celecoxib)	96	145
8	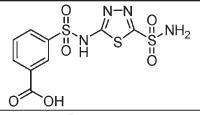	3-(5-sulfamoyl-1,3,4-thiadiazol-2-ylsulfamoyl)-benzoic acid	31	16
9	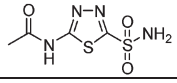	2-acetylamido-1,3,4-thiadiazole-5-sulfonamide (Acetazolamide)	2	8

Since different carbonic anhydrase isoenzymes are involved in many physiological and pathological processes, they have been interesting therapeutical targets for treatment of many well-known diseases such as Alzheimer's disease, edema, glaucoma, cancer, epilepsy, obesity, and osteoporosis (*13*, *14*). Herein we present a small-molecule inhibitor survey with selected sulfonamide inhibitors of varying potency to investigate the effectiveness of these molecules to prevent the misfolding of HCA II_{H107Y} *in vitro*. We also demonstrate that high concentrations of the activator compound L-His increase the enzyme activity of the mutant but without stabilizing the folded protein. This study provides a starting point for the design of small-molecule misfolding inhibitors to function as "pharmacological chaperones" of HCA II mutants prone to misfold. This apparently contradictory strategy has proven successful in other loss-of-function enzyme deficiencies (*15*, *16*).

MATERIALS AND METHODS

Chemicals. Ultrapure GuHCl was obtained from MP Biochemicals, and the concentration of all GuHCl solutions was determined refractometrically (*17*).

Isopropyl β-D-thiogalactopyranoside (IPTG) was purchased from Saveen, and 8-anilino-1-naphthalenesulfonic acid (ANS) was obtained from Sigma. The structures of the nine sulfonamide inhibitors used are shown in Table 1. Inhibitors **1**−**6** and **8** were synthesized as described previously (*18*−*20*), and inhibitor **7** (celecoxib) was obtained as described previously (*21*). Inhibitor **9** (acetazolamide) was obtained from Sigma.

Production of Protein. HCA II_{H107Y} was expressed and purified as previously described by us (*10*). The template was the cysteine-free variant HCA II_{C206S}, and we have previously shown that this pseudo wild type (HCA II_{pwt}) has properties indistinguishable from those of the wild type (*22*).

Activity Measurements. The CO_2 hydration activity for HCA II_{pwt} and HCA II_{H107Y} was determined by the colorimetric method of Rickli et al. at 0 °C (*23*), in order to obtain the inhibitory concentration at 50% enzyme activity (IC_{50}). To determine the IC_{50} values for the different inhibitors, appropriate amounts of inhibitor (inhibitor stock solutions of 10 mM in DMSO) were added to the enzyme in the assay solution and allowed to incubate for 1 min before the addition of the CO_2 substrate. Solvent effects on the enzyme activity were adjusted for.

The different activators (L-His, L-Phe, and D-Phe, stock solution of 1 mM in distilled H_2O) were added in 750-fold molar excess over the enzyme to determine their ability to increase the activity of both HCA II_{pwt} and HCA II_{H107Y}. The activators were incubated for 1 min with the enzyme before the addition of the CO_2 substrate.

Stability Measurements. The stability toward GuHCl denaturation was followed by changes in the intrinsic fluorescence at 4 °C. The protein variants (0.8 μM in 100 mM sodium borate, pH 7.5) were incubated for 20 h at 4 °C at various concentrations of GuHCl and also in the presence of the different inhibitors in a final concentration of 10 μM. The fluorescence spectra were recorded on a Hitachi F-4500 using a thermostated cell, which kept the temperature at 4 °C. The path length was 1 cm, and both the entrance and exit slits were set to 5 nm. Excitation wavelength was 295 nm, and the spectra were recorded between 310 and 450 nm.

The data were fitted to two separate unfolding transitions for calculation of the Gibbs free energy of unfolding for the transitions from the native, N, to the intermediate, I, and from the I to the unfolded, U, state, respectively ($\Delta G_{N\rightarrow I}$ and $\Delta G_{I\rightarrow U}$) in order to normalize the two unfolding transitions. The first unfolding transition in GuHCl which corresponds to the thermal unfolding transition represents unfolding of the folded state to the molten globule light/molten globule state denotes the stability of the native protein (*10*). A linear dependence of the GuHCl concentration of the Gibbs free energy of unfolding was assumed for both transitions (*24*). The free energy of unfolding of the native state was calculated according to the formula:

$$\Delta G_{N\rightarrow I} = \Delta G_{N\rightarrow I}{}^{H_2O} - m_{N\rightarrow I}[\mathrm{GuHCl}] \quad (1)$$

where ΔG^{H_2O} denotes the Gibbs free energy of unfolding of the mutant in the absence of denaturant and $m_{N\rightarrow I}$ denotes the slope of the dependence of the stability on denaturant concentration which reflects the cooperativity of folding and is proportional to the exposure of solvent-accessible surface area (*25*).

The thermal stability of the protein variants (0.8 μM in 100 mM sodium borate, pH 7.5), both in the presence and in the absence of the inhibitors at two different final concentrations (0.8 and 10 μM), was measured as described previously (*10*).

The thermal stability for HCA II_{H107Y} (0.8 μM in 100 mM sodium borate, pH 7.5) was also determined in the absence and presence of three different activators (pH 8.0) at a final concentration of 10 μM. Samples were incubated overnight at 4 °C, and the measurements were performed as described previously (*10*).

A consequence of inhibitor binding to HCA II_{H107Y} is that the inhibitor binds tightly to the fully folded conformation rather than to the unfolded state and any distorted or partially unfolded intermediate forms. This can be illustrated by the following equation for the free energy of binding (ΔG_b):

$$\Delta G_b = -RT \ln([A]/K_d) \quad (2)$$

where [A] is the concentration of free inhibitor and K_d is the dissociation constant. With a concentration equal of K_d half the protein molecules have bound inhibitor. This theoretical binding energy was calculated for all inhibitors simply assuming the obtained IC_{50} values as K_d values in order to compare the theoretical binding energies with obtained experimental stability data.

Thermal Stability Kinetics. The kinetic resistance toward thermal denaturation was measured for the enzyme variants with and without the different activators. The enzymes (0.8 μM in 100 mM sodium borate, pH 8.0) were incubated with activators (final concentration of 600 μM) at 4 °C for 10 min. The samples were then transferred to 37 °C using a heating block, and the activity was monitored every 30 s using the CO_2 hydration assay (*18*).

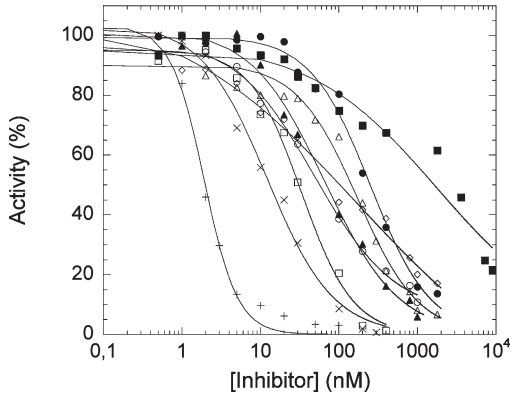

FIGURE 1: Inhibition of CO_2 hydration activity of HCA II_{H107Y} by different sulfonamide compounds: (●) inhibitor **1**; (○) inhibitor **2**; (▲) inhibitor **3**; (△) inhibitor **4**; (■) inhibitor **5**; (×) inhibitor **6**; (◊) inhibitor **7**; (□) inhibitor **8**; (+) inhibitor **9**.

RESULTS

Inhibition of Enzyme Activity. We measured the efficiency of the nine sulfonamide compounds to inhibit the CO_2 hydration activity to obtain the inhibitory concentration at 50% enzyme activity, IC_{50}. The compounds were selected to range between poor to very good inhibitors and showed a range of IC_{50} values from 1640 nM (**5**) to 2 nM (**9**) (Table 1, Figure 1) against HCA II_{H107Y}. The IC_{50} values of the compounds to inhibit the mutant and the pseudo-wild-type enzyme followed a similar efficiency pattern.

Stabilization. To determine the stabilization capability of the different inhibitors at pH 7.5, we measured the stability, by the change in intrinsic Trp fluorescence, toward both GuHCl denaturation at 4 °C and thermal denaturation. Due to the high number of Trps in HCA II, and the even distribution thereof, this is a sensitive method to monitor the global unfolding of the protein (*26*). By thermal unfolding HCA II can be unfolded to an intermediate (I) of molten globule type (*10*, *27*, *28*). For GuHCl unfolding HCA II unfolds in two cooperative transitions: (i) from the native state (N) to an intermediate state (I) and (ii) from the intermediate to the unfolded state. The thermally accessible intermediate corresponds well to the intermediate at moderate concentrations of GuHCl (*27*, *28*), but furthermore severely destabilized mutants of HCA II (such as H107Y) also populate a more native-like intermediate abbreviated molten globule light state (*10*, *11*). All unfolding curves both in the presence and in the absence of inhibitor showed similar unfolding trajectories (Figure 2), but with higher midpoints of thermal denaturation (T_m) and midpoint concentrations of GuHCl denaturation (C_m) compared to the corresponding values of the unliganded mutant. A net stabilization effect toward both chemical and thermal denaturation was observed for all inhibitors but to various degrees (Figure 2, Table 2). For GuHCl denaturation Figure 2C shows the transitions from the native state to the intermediate state, which represents the unfolding of the native structure. The efficacy in stabilizing HCA II_{H107Y} ranged from upward shifts in T_m with 1−11 °C at 1:1 inhibitor:enzyme ratio

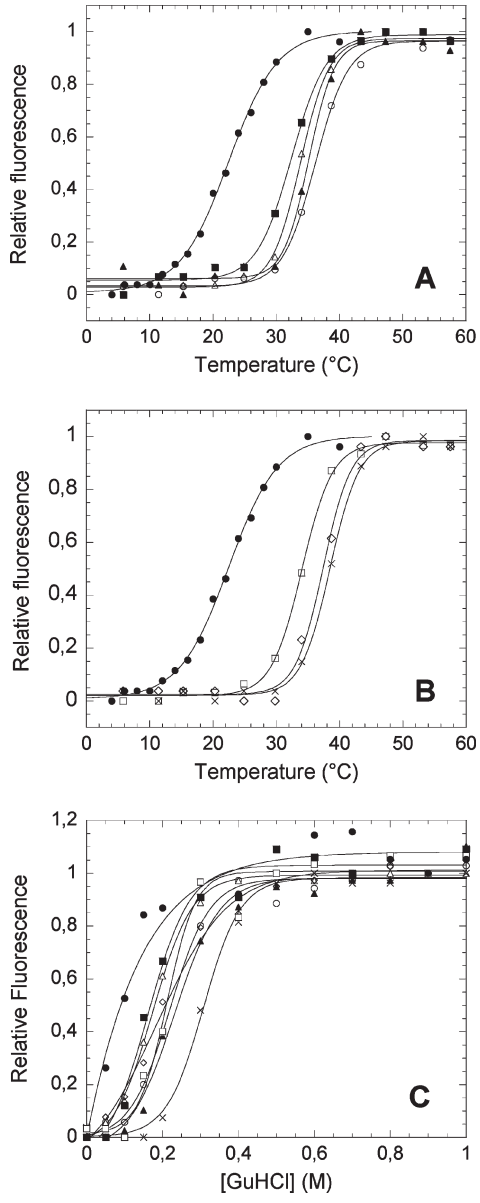

FIGURE 2: (A, B) Stability of HCA II_{H107Y} toward thermal denaturation. The enzyme concentration was 0.8 μM in 100 mM sodium borate, pH 7.5, and the final concentration of the inhibitors was 10 μM. (C) Stability of HCA II_{H107Y} toward denaturation by GuHCl at 4 °C. The figure shows the unfolding transition from native state to the intermediate state. The enzyme concentration was 0.8 μM in 100 mM sodium borate, pH 7.5, and the final concentration of the inhibitors was 10 μM. Key: (●) no inhibitor; (○) inhibitor **2**; (▲) inhibitor **3**; (△) inhibitor **4**; (■) inhibitor **5**; (×) inhibitor **6**; (◊) inhibitor **7**; (□) inhibitor **8**.

(0.8 μM inhibitor) to T_m shifts of 10−16 °C for 12:1 inhibitor:enzyme ratio (Table 2). The results from the thermal denaturation experiments when the inhibitors were in a 12-fold molar excess over enzyme are shown in Figure 2A,B. When the protein was subjected to GuHCl denaturation, stability data were obtained for 12:1 inhibitor:enzyme ratio (10 μM inhibitor) and provided a net stabilization of 0.5−3.0 kcal/mol (Figure 2C, Table 2).

Activation and Thermal Stability in the Presence of HCA II Activators. We also investigated the influence on HCA II_{H107Y} of different known HCA II activators, L-His, L-Phe, and D-Phe, that have been shown to bind to the outer rim of the active site of HCA II (*29*, *30*). Activators applied at high concentrations (600 μM) increased the CO_2 hydration activity of HCA II_{H107Y} to 162% for L-His. However, neither L-Phe nor D-Phe increased the enzyme activity of HCA II_{H107Y}. The thermal stability was measured for HCA II_{H107Y} with the three activators present in a 12-fold molar excess (10 μM) at pH 8.0. Even though the activator molecule L-His is known to bind with moderate affinity to HCA II (a reported 50% of the total increase in activity at 10.9 μM, called "activation constant") (*29*), no stabilizing effect was detected at 10 μM of neither L-His, L-Phe, nor D-Phe, and hence the T_m values for the different experiments were indistinguishable (26 ± 1 °C) from the control where no activator was present (Figure 3, inset).

We thereafter investigated if the binding of the activators could slow the kinetics of thermal unfolding. At 37 °C the enzyme activity was lost within a few minutes for the unliganded HCA II_{H107Y} (Figure 3). The activation effect when L-His was present in a 750-fold molar excess (600 μM) did not alter the decay rate of the activity for the enzyme, neither did addition of the D- or L-Phe (600 μM) influence the thermal denaturation kinetics (Figure 3).

DISCUSSION

In this work a number of different HCA II aromatic sulfonamide inhibitors and amino acid activators were selected to assess their potency for stabilizing the protein and thereby prevent misfolding of the CADS-associated mutant HCA II_{H107Y}. The selection was performed in order to have a wide spectrum of poor to very strong binders to address whether the expected strong inhibitors also were superior misfolding inhibitors. Stability was assessed both in the absence of denaturant by thermal denaturation, reflecting the most physiological setting, and in the presence of a denaturant, GuHCl, at low temperatures.

The different inhibitors tested in this study showed similar inhibition effect for both the pseudo-wild type enzyme and the mutant HCA II_{H107Y}. The active site appears rather

Table 2: Stability Data of Unfolding of the Native State of HCA II_{H107Y} in the Presence of Compounds **2**−**9**

compd	C_m[a] N→I (M)	ΔC_m N→I (M)	ΔG_{H_2O} N→I (kcal/mol)	$\Delta\Delta G_{H_2O}$ N→I (kcal/mol)	T_m[b] 1:1 (°C)	ΔT_m 1:1 (°C)	T_m 12:1 (°C)	ΔT_m 12:1 (°C)
	0.09		1.1		22		22	
2	0.24	0.15	2.8	−1.7	31	9	36	14
3	0.22	0.13	2.2	−1.1	30	8	35	13
4	0.18	0.09	2.1	−1.0	30	8	34	12
5	0.19	0.10	1.9	−0.8	23	1	32	10
6	0.32	0.23	3.7	−2.6	29	7	38	16
7	0.20	0.11	1.6	−0.5	29	7	37	15
8	0.21	0.12	2.3	−1.2	29	7	34	12
9	0.28[c]	0.24[c]	3.4[c]	−3.0[c]	33	11	34[c]	16[c]

[a] C_m = midpoint concentration of GuHCl denaturation. [b] T_m = midpoint of thermal denaturation. [c] The data for inhibitor **9** (acetazolamide) are from our previous study (*10*), where the drug was dissolved in EtOH.

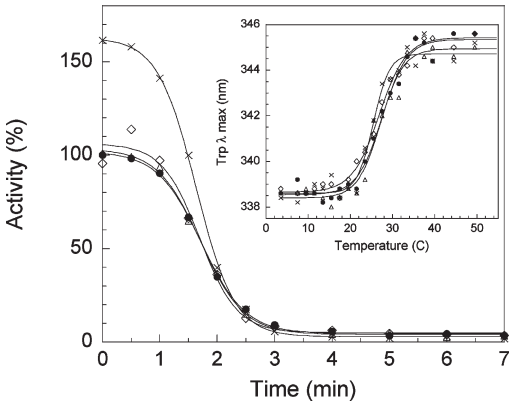

FIGURE 3: Thermal stability kinetics for HCA II_{H107Y} with different activators. The enzyme was incubated with the activator for 10 min at 4 °C and the sample was then transferred to 37 °C, and the decay in activity was monitored. The enzyme concentration was 0.8 μM in 100 mM sodium borate, pH 8.0; the final concentration of the activators was 600 μM. The inset shows temperature denaturation curves for HCA II_{H107Y} (0.8 μM) with different activators (10 μM) in 100 mM sodium borate, pH 8.0. Activity decay curves and inset: (●) no activator; (×) L-His; (◊) L-Phe; (△) D-Phe.

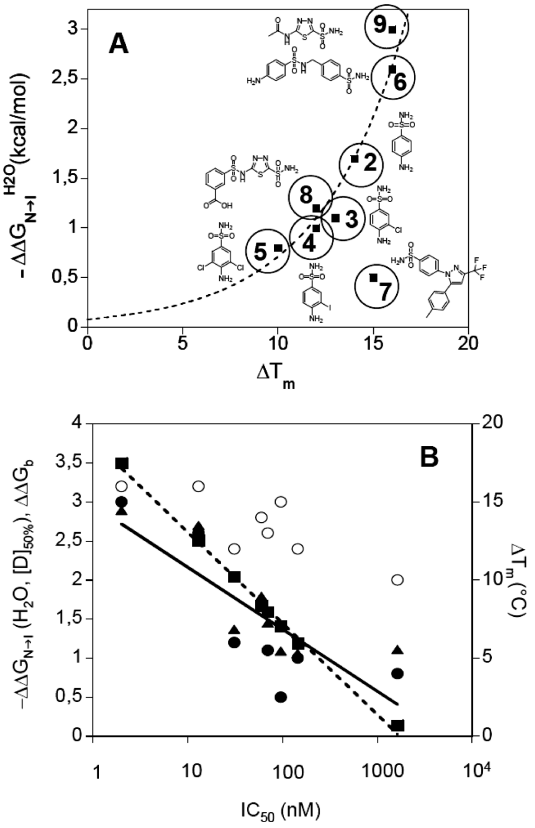

FIGURE 4: (A) Correlation between the inhibitor-induced stabilization effects of GuHCl determined stability (4 °C) expressed as the change in free energy of unfolding of the native state ($-\Delta\Delta G_{N\rightarrow I}^{H_2O}$) and the change of thermal stability (ΔT_m) (in °C) of the first unfolding transition of HCA II_{H107Y} in the presence of the different inhibitors. The dashed line was drawn to guide the eye. The enzyme concentration was 0.8 μM in 100 mM sodium borate, pH 7.5; the final concentration of the inhibitors was 10 μM. (B) Correlation between the inhibitor-induced stabilization effects of GuHCl determined stability (4 °C) extrapolated to water ($-\Delta\Delta G_{N\rightarrow I}^{H_2O}$) and at the midpoint concentration of denaturant ($-\Delta\Delta G_{N\rightarrow I}[D]_{50\%}$) (in kcal/mol) to accommodate *m*-value differences; the calculated free energy of binding ($-\Delta\Delta G_b$) (estimating IC_{50} values to correspond to K_d values) and the thermal stability (ΔT_m) of HCA II_{H107Y} in the first unfolding transition versus the IC_{50} values for the different inhibitors on a logarithmic scale. Key: (●) $-\Delta\Delta G_{N\rightarrow I}^{H_2O}$ (kcal/mol); (▲) $-\Delta\Delta G_{N\rightarrow I}[D]_{50\%}$ (kcal/mol); (■) $-\Delta\Delta G_b$ (kcal/mol); (○) ΔT_m (°C). The solid line shows the fit of the theoretical binding induced stability (r = 0.997) and the dashed line shows the fit to the experimental binding and stability at the two different GuHCl concentrations (r = 0.817).

accommodating toward different sizes of the bound aromatic sulfonamides. The potency and structure−activity relationship (SAR) of aromatic sulfonamides for inhibition of HCA II have been discussed extensively in the literature (*14*). Herein we will limit this discussion to the efficacy of these molecules toward stabilization of the misfolding prone HCA II_{H107Y} mutant and reflect their stabilizing effect on the inhibitory potency. There was a clear stabilizing effect of all aromatic sulfonamides versus both thermal and chemical denaturation. A correlation diagram of the increase in free energy of unfolding at 4 °C by GuHCl denaturation versus increase in T_m at excess compound displayed an interesting correlation between these independently assayed parameters of inhibitor-induced stability (Figure 4A). We have previously demonstrated a linear correlation between these parameters over a much wider range of temperatures for different HCA II mutants (*11*), indicating that point mutations do not significantly change the heat capacity but merely shifts the free energy of unfolding in parallel with temperature. The nonlinear correlation of the thermal and GuHCl stabilizing effects of the inhibitors in the study suggests that ionic modulation by GuHCl can render binding-induced folding less efficient for the inhibitors at 4 °C. In contrast, the thermal stability, which improved significantly for all inhibitors, appears to be facilitated by hydrophobic interactions because these are assayed at a higher temperature range (25−40 °C). It was rather striking that even the poorest inhibitor shifted the T_m by 10 °C (Figure 4).

First we focus on the amino-substituted benzoylsulfonamides, compounds **1**−**5**. Unfortunately, the stability in the presence of inhibitor **1** could not be measured due to intrinsic fluorescence of **1** when bound to HCA II interfering with the Trp fluorescence spectrum (data not shown). Nevertheless, we obtained reliable data for all other inhibitors. Molecules **2**−**5** are simple *p*-aminobenzoylsulfonamide compounds. Introducing a halo substituent in the meta position lowers the stabilizing effect both versus thermal and versus chemical denaturation. Chloride (**3**) was more acceptable than iodide (**4**), but a double substitution was less acceptable (**5**). This relation was also reflected in the IC_{50} values, which decrease in parallel with the increased stabilizing effects.

The more complex inhibitors **6** and **7** are also analogous para-substituted benzoylsulfonamides. Compound **6** has a methyl spacer prior to the adjacent *p*-aminobenzoylsulfonamide substitution. Evidently the double aromatic sulfonamide (**6**) renders the compound a significantly more potent inhibitor (cf. IC_{50} of **2**, Table 1) and, moreover, renders this molecule a more potent stabilizing molecule, in particular versus chemical denaturation. In contrast, the large bulky compound **7**, which has a higher IC_{50} value compared to compound **2**, shows a higher potency than compound **2** against thermal denaturation but a significantly lower stabilizing effect against chemical denaturation. Evidently the correlation for inhibitor **7** is very poor for stabilization toward thermal and chemical denaturation and when comparing this molecule with the other para-substituted benzoylsulfonamides (Figure 4A). Compound **7** (celecoxib) is unusual compared to the other compounds in the study, and rather variable

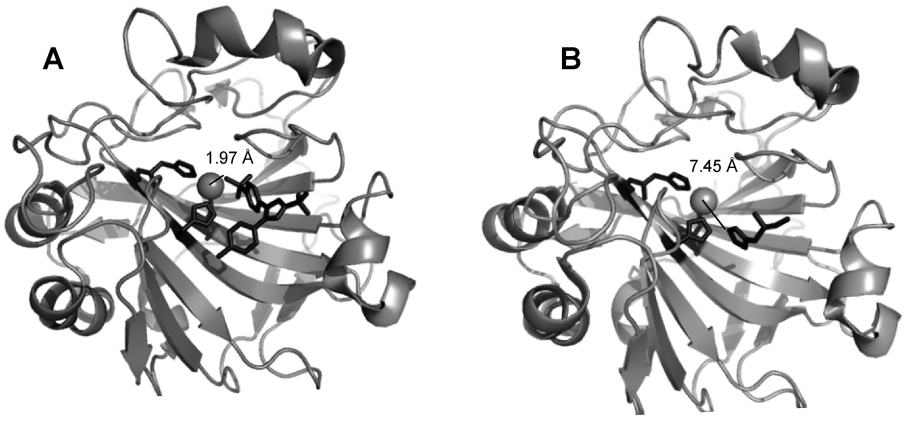

FIGURE 5: (A) Crystal structure of the complex between HCA II and inhibitor **7**. Residues H94, H96, and H119 and the inhibitor are shown as stick models, and the Zn^{2+} ion is shown as a sphere. The distance between the zinc ion and the nitrogen in the sulfonamide nitrogen is 1.97 Å. The figure was generated in Pymol, using the PDB code 1OQ5 (*31*). (B) Crystal structure of the complex between HCA II and the activator L-His. Residues H94, H96, H119, and L-His are shown as stick models, and the Zn^{2+} ion is shown as a sphere. L-His binds to the rim of the active site, and the distance between the zinc ion and the closest located imidazole nitrogen is 7.45 Å. The figure was generated in Pymol, using the PDB code 2ABE (*30*).

inhibition constants have been reported which are in the range of 21−410 nM (*21*, *31*), likely arising from various assay methods and incubation times. The molecule binds in a rather standard fashion to HCA II as shown in the crystal structure (Figure 5A) (*31*) with the expected binding of the sulfonamide to the Zn^{2+} ion in the active site.

We also included two 1,3,4-thiadiazolylsulfonamides in the study (compounds **8** and **9**). Here it was striking how the smaller compound **9** (acetazolamide) was a much more potent inhibitor and a much more effective stabilizing molecule than compound **8**. Also, here the IC_{50} value obtained for compound **8** rather poorly reflects its effectiveness as a stabilizing molecule. If the IC_{50} value would be the predictor of stabilizing capacity, compound **8** would be the third best stabilizing molecule. It is only the fourth best compound for chemical denaturation and is at a shared sixth place for thermal stability. In the correlation diagram (Figure 4A) compound **8** groups with compounds **3** and **4**, which both are less potent inhibitors than compound **8**.

In the perfect scenario a misfolding inhibitor should stabilize the protein so that the T_m is above 37 °C but at the same time have an IC_{50} value that allows a fraction of the enzyme molecules to be free of inhibitor, or to be out-competed by substrate, to allow catalysis. In this case where the disease mutant is so strongly destabilized, only the most potent drugs were able to stabilize the protein to such a high degree that half of the protein molecules were in the native form at 37 °C. But here we pay the price of losing the enzyme activity due to the high concentration of inhibitor demanded to get this stabilization effect. This appears to be an impossible scenario from a thermodynamic consideration of the shift of the equilibrium toward the inhibited liganded native state of the enzyme. Nevertheless, it has been shown for the lyosomal storage diseases, Fabry's disease and Gaucher's disease, that active site directed inhibitors of both α-galactosidase A and glucocerebrosidase could bind to and stabilize the mutant enzymes in the endoplasmic reticulum (ER), enabling their trafficking to the lysosome rendering elevated enzyme activity in this organelle (*15*, *16*, *32*). This concept has been referred to as "pharmacological chaperoning". In these cases the mechanism of inhibitor dissociation following binding in the neutral pH of the ER was facilitated by the low pH of the lysosome and the concurrent presence of excess substrate (*33*). HCA II_{H107Y} fulfills the most important criterion for the "pharmacological chaperoning" mechanism to be successful, i.e., an enzyme which is foldable to the active conformation. Potential candidates for affording a partial restoration behavior for HCA II_{H107Y} at modest inhibition levels are compounds **4** and **7**, which increase T_m to the same extent as more potent inhibitors both at 0.8 and at 10 μM concentration of inhibitor despite showing higher IC_{50} values (Table 2). We also investigated the activator compound L-His which was rather potent in increasing the enzyme activity at high concentrations, however, unfortunately with no stabilizing effect on the protein. That both D- and L-Phe were incapable of increasing the activity of HCA II_{H107Y} indicates that the binding site in the mutant is different from the wild-type site, likely originating from a more labile site in the mutant compared to the wild-type protein. In light of the stabilizing efficacy of sulfonamide inhibitors this indicates that shifting the equilibrium toward the native state necessitates a firm anchoring site in HCA II, a characteristic lacking for the activator binding site, at the outer rim of the active site which is located at a 4-fold longer distance for L-His compared to a sulfonamide (Figure 5B) (*29*).

The stabilization effects demonstrated toward both chemical and thermal denaturation correlate well for all compounds (except for compound **7**) (Figure 4A), indicating that the shift of stability reflects the stabilization of the native state. Hence, this is an expected action of a site-specific inhibitor induced shift of the equilibrium toward the liganded native state. It was however unexpected that the relation between these different stability parameters was nonlinear and that the linear correlation between the binding affinities (IC_{50} values) and the stabilization capacity of the inhibitors, shown in Figure 4B, was fairly poor (r = 0.817) in relation to the theoretical binding efficiency estimating IC_{50} values to correspond to dissociation constants (r = 0.997).

In this report we have shown the first example of how small-molecule inhibitors and activators of various affinities stabilized the mutated HCA II. Aromatic sulfonamide inhibitors buried deep in the active site bound to the Zn ion can rather efficiently shift the equilibrium toward the native state of HCA II_{H107Y}. This study could be used as a starting point for design of folding modulating small molecules and possibly autoactivatable molecules for suppression of misfolding of destabilized HCA II mutants.

ACKNOWLEDGMENT

We thank Patricia Wennerstrand for assistance with graphics.

REFERENCES

1. Gregersen, N., Bross, P., Vang, S., and Christensen, J. H. (2006) Protein misfolding and human disease. *Annu. Rev. Genomics Hum. Genet. 7*, 103–124.
2. Sanyal, G., and Maren, T. H. (1981) Thermodynamics of carbonic anhydrase catalysis. A comparison between human isoenzymes B and C. *J. Biol. Chem. 256*, 608–612.
3. Lindskog, S. (1997) Structure and mechanism of carbonic anhydrase. *Pharmacol. Ther. 74*, 1–20.
4. Wistrand, P. J. (1981) The importance of carbonic anhydrase B and C for the unloading of CO2 by the human erythrocyte. *Acta Physiol. Scand. 113*, 417–426.
5. Sly, W. S., Hewett-Emmett, D., Whyte, M. P., Yu, Y. S., and Tashian, R. E. (1983) Carbonic anhydrase II deficiency identified as the primary defect in the autosomal recessive syndrome of osteopetrosis with renal tubular acidosis and cerebral calcification. *Proc. Natl. Acad. Sci. U.S.A. 80*, 2752–2756.
6. Hakansson, K., Carlsson, M., Svensson, L. A., and Liljas, A. (1992) Structure of native and apo carbonic anhydrase II and structure of some of its anion-ligand complexes. *J. Mol. Biol. 227*, 1192–1204.
7. Shah, G. N., Bonapace, G., Hu, P. Y., Strisciuglio, P., and Sly, W. S. (2004) Carbonic anhydrase II deficiency syndrome (osteopetrosis with renal tubular acidosis and brain calcification): novel mutations in CA2 identified by direct sequencing expand the opportunity for genotype-phenotype correlation. *Hum. Mutat. 24*, 272.
8. Venta, P. J., Welty, R. J., Johnson, T. M., Sly, W. S., and Tashian, R. E. (1991) Carbonic anhydrase II deficiency syndrome in a Belgian family is caused by a point mutation at an invariant histidine residue (107 His→Tyr): complete structure of the normal human CA II gene. *Am. J. Hum. Genet. 49*, 1082–1090.
9. Soda, H., Yukizane, S., Yoshida, I., Koga, Y., Aramaki, S., and Kato, H. (1996) A point mutation in exon 3 (His 107→Tyr) in two unrelated Japanese patients with carbonic anhydrase II deficiency with central nervous system involvement. *Hum. Genet. 97*, 435–437.
10. Almstedt, K., Lundqvist, M., Carlsson, J., Karlsson, M., Persson, B., Jonsson, B. H., Carlsson, U., and Hammarstrom, P. (2004) Unfolding a folding disease: folding, misfolding and aggregation of the marble brain syndrome-associated mutant H107Y of human carbonic anhydrase II. *J. Mol. Biol. 342*, 619–633.
11. Almstedt, K., Martensson, L. G., Carlsson, U., and Hammarstrom, P. (2008) Thermodynamic interrogation of a folding disease. Mutant mapping of position 107 in human carbonic anhydrase II linked to marble brain disease. *Biochemistry 47*, 1288–1298.
12. Maren, T. H. (1967) Carbonic anhydrase: chemistry, physiology, and inhibition. *Physiol. Rev. 47*, 595–781.
13. Supuran, C. T. (2008) Carbonic anhydrases: novel therapeutic applications for inhibitors and activators. *Nat. Rev. Drug Discovery 7*, 168–181.
14. Supuran, C. T., Scozzafava, A., and Casini, A. (2003) Carbonic anhydrase inhibitors. *Med. Res. Rev. 23*, 146–189.
15. Sawkar, A. R., Cheng, W.-C., Beutler, E., Wong, C.-H., Balch, W. E., and Kelly, J. W. (2002) Chemical chaperones increase the cellular activity of N370S _-glucosidase: a therapeutic strategy for Gaucher disease. *Proc. Natl. Acad. Sci. U.S.A. 99*, 15428–15433.
16. Yam, G. H-F., Zuber, C., and Roth, J. (2005) A synthetic chaperone corrects the trafficking defect and disease phenotype in a protein misfolding disorder. *FASEB J. 19*, 12–18.
17. Nozaki, Y. (1972) The preparation of guanidine hydrochloride. *Methods Enzymol. 26* (Part C), 43–50.
18. Casini, A., Scozzafava, A., Mincione, F., Menabuoni, L., Starnotti, M., and Supuran, C. T. (2003) Carbonic anhydrase inhibitors: topically acting antiglaucoma sulfonamides incorporating esters and amides of 3- and 4-carboxybenzolamide. *Bioorg. Med. Chem. Lett. 13*, 2867–2873.
19. Ilies, M. A., Vullo, D., Pastorek, J., Scozzafava, A., Ilies, M., Caproiu, M. T., Pastorekova, S., and Supuran, C. T. (2003) Carbonic anhydrase inhibitors. Inhibition of tumor-associated isozyme IX by halogenosulfanilamide and halogenophenylaminobenzolamide derivatives. *J. Med. Chem. 46*, 2187–2196.
20. Clare, B., and Supuran, C. (1999) Carbonic anhydrase inhibitors. Part 61. Quantum chemical QSAR of a group of benzenedisulfonamides. *Eur. J. Med. Chem. 34*, 463–474.
21. Knudsen, J. F., Carlsson, U., Hammarstrom, P., Sokol, G. H., and Cantilena, L. R. (2004) The cyclooxygenase-2 inhibitor celecoxib is a potent inhibitor of human carbonic anhydrase II. *Inflammation 28*, 285–290.
22. Martensson, L. G., Jonsson, B. H., Freskgard, P. O., Kihlgren, A., Svensson, M., and Carlsson, U. (1993) Characterization of folding intermediates of human carbonic anhydrase II: probing substructure by chemical labeling of SH groups introduced by site-directed mutagenesis. *Biochemistry 32*, 224–231.
23. Rickli, E. E., Ghazanfar, S. A., Gibbons, B. H., and Edsall, J. T. (1964) Carbonic anhydrases from human erythrocytes. Preparation and properties of two enzymes. *J. Biol. Chem. 239*, 1065–1078.
24. Bolen, D. W., and Santoro, M. M. (1988) Unfolding free energy changes determined by the linear extrapolation method. 2. Incorporation of delta G degrees N-U values in a thermodynamic cycle. *Biochemistry 27*, 8069–8074.
25. Myers, J. K., Pace, C. N., and Scholtz, J. M. (1995) Denaturant m values and heat capacity changes: relation to changes in accessible surface areas of protein unfolding. *Protein Sci. 4*, 2138–2148.
26. Martensson, L. G., Jonasson, P., Freskgard, P. O., Svensson, M., Carlsson, U., and Jonsson, B. H. (1995) Contribution of individual tryptophan residues to the fluorescence spectrum of native and denatured forms of human carbonic anhydrase II. *Biochemistry 34*, 1011–1021.
27. Persson, M., Hammarstrom, P., Lindgren, M., Jonsson, B. H., Svensson, M., and Carlsson, U. (1999) EPR mapping of interactions between spin-labeled variants of human carbonic anhydrase II and GroEL: evidence for increased flexibility of the hydrophobic core by the interaction. *Biochemistry 38*, 432–441.
28. Hammarstrom, P., Persson, M., and Carlsson, U. (2001) Protein compactness measured by fluorescence resonance energy transfer. Human carbonic anhydrase ii is considerably expanded by the interaction of GroEL. *J. Biol. Chem. 276*, 21765–21775.
29. Temperini, C., Scozzafava, A., Vullo, D., and Supuran, C. T. (2006) Carbonic anhydrase activators. Activation of isozymes I, II, IV, VA, VII, and XIV with L- and D-histidine and crystallographic analysis of their adducts with isoform II: engineering proton-transfer processes within the active site of an enzyme. *Chemistry (Weinheim, Germany) 12*, 7057–7066.
30. Temperini, C., Scozzafava, A., Vullo, D., and Supuran, C. T. (2006) Carbonic anhydrase activators. Activation of isoforms I, II, IV, VA, VII, and XIV with L- and D-phenylalanine and crystallographic analysis of their adducts with isozyme II: stereospecific recognition within the active site of an enzyme and its consequences for the drug design. *Journal of medicinal chemistry 49*, 3019–3027.
31. Weber, A., Casini, A., Heine, A., Kuhn, D., Supuran, C. T., Scozzafava, A., and Klebe, G. (2004) Unexpected nanomolar inhibition of carbonic anhydrase by COX-2-selective celecoxib: new pharmacological opportunities due to related binding site recognition. *J. Med. Chem. 47*, 550–557.
32. Zhanqian, Y., Sawkar, A. R., and Kelly, J. W. (2007) Pharmacologic chaperoning as a strategy to treat Gaucher disease. *FEBS J. 274*, 4944–4950.
33. Sawkar, A. R., Schmitz, M., Zimmer, K.-P., Reczek, D., Edmunds, T., Balch, W. E., and Kelly, J. W. (2006) Chemical chaperones and permissive temperatures alter the cellular localization of gaucher disease associated glucocerebrosidase variants. *ACS Chem. Biol. 1*, 235–251.